

## X-ray scattering from laser-shock driven plasmas

F Y Khattak, K A Thornton, D Riley

School of Mathematics and Physics, Queen's University of Belfast, University Road, Belfast, BT7 1NN, UK

C D Gregory, N C Woolsey

Department of Physics, University of York, Heslington, York, YO10 5DD, UK

M Notley, D Neely

Central Laser Facility, CCLRC Rutherford Appleton Laboratory, Chilton, Didcot, Oxon., OX11 0QX, UK

Main contact email address: f.khattak@qub.ac.uk

### Introduction

The subject of Warm Dense Matter (WDM)<sup>1</sup> has been actively pursued by plasma-physicists because laboratory laser-plasmas, at some stage, pass through this regime and equally by geo-physicists due to the occurrence of these systems in the core of giant planets. Such systems are strongly coupled as quantified by the strong coupling parameter defined as:  $\Gamma_{II} = (Z^*e)^2 / (R\kappa_B T_I)$ , where  $Z^*e$  is the ion net charge,  $R$  is the ion sphere radius [ $R = (3/4\pi n_I)^{1/3}$  with  $n_I$  the ion number density], and  $T_I$  is the ion temperature. For  $\Gamma_{II} > 1$ , the Coulomb potential exceeds the thermal energy and the Debye-Huckel treatment is no longer valid. Such systems can also not be explained by the solid state models which assume a temperature less than the Fermi temperature.

In laser-shock driven plasmas, the ions are heated first and then electrons absorb energy from the ions within a characteristic equilibration time. In classical plasma the equilibration time could be very short compared to the typical timescale of experiments. Since the lower energy states are no longer available for the electrons to scatter into, degeneracy effects increase this time scale. Even so, for an aluminium plasma at solid density, an electron temperature of 3eV and ion temperature of 0.081eV (melting temperature), the Spitzer-Brysk model (SB)<sup>2,3</sup> predicts a coupling rate of the order of  $10^{18} \text{W/K/m}^3$  (using the perfect gas heat capacity,  $3k_B n_I/2$ , for the ions). This amounts to a sub-picosecond equilibration time. In strongly coupled plasma, the electrons collide with coupled groups of ions and the increased effective mass ratio reduces the energy exchange rate. Dharma-Wardana and Perrot models<sup>4</sup> employing a quantum mechanical approach, predict a coupling rate of  $10^{17} \text{W/K/m}^3$  for weak electron-ion coupling and  $10^{16} \text{W/K/m}^3$  for dynamically dependent species. This makes the equilibration time tens of picoseconds. Experimental studies of such systems are difficult as they require diagnosing and producing these extreme conditions simultaneously. An experimental campaign carried out by Celliers *et al.*<sup>5</sup> and Ng *et al.*<sup>6</sup>, looking at the optical emission from the rear of the laser shocked silicon, shows signatures of slow electron heating. In their case, ions were heated first.

We report here on an experiment that is part of our campaign to establish the technique of x-ray scattering<sup>7-9</sup> for studying the electron ion equilibration. This technique is based on coherent scattering from ions that retain a large number of bound electrons. The spectrally integrated scatter varies as a function of angle in a manner similar to a liquid metal<sup>10</sup>. The shape of the cross section versus angle is dominated by the ion-ion structure factor, which depends intimately on the ion-ion coupling parameter. The position of the peak could be used as a diagnostic for the direct measurement of the plasma density.

### Experimental arrangements

The experiment was performed at the Rutherford Appleton Laboratory using the multi-beam laser facility Vulcan in Target Area East. A schematic of the experiment is shown in Figure 1. The main six beams, delivering ~200J in IR, were frequency doubled to 527nm and synchronously focused to an overlapping

spot of ~3mm on the main plasma target. The principal focusing optics, f/10 lens, was used in conjunction with a 3mm Binary-Phase Zone Plates (PZP)<sup>11</sup> on the main beams. This produces almost flat-top intensity distribution on target with a central spike. The lenses were offset by 5mm from the best focus to reduce the level of the associated central spike.

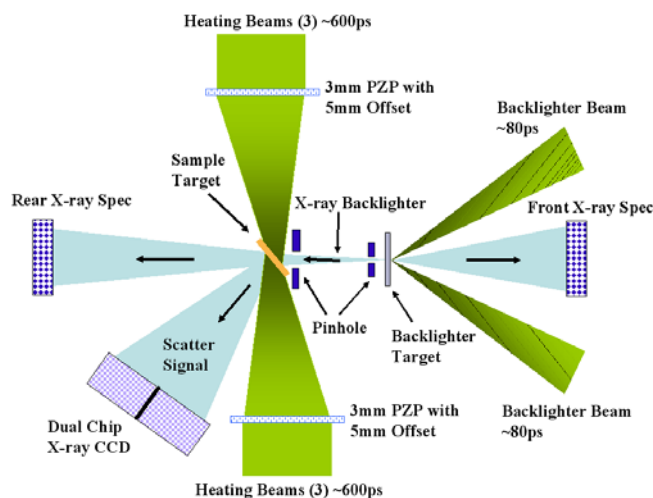


Figure 1. A schematic of the experimental layout.

The pulse shape of the main beam, recorded with an optical streak camera, shows a fast rise (~200ps) but a very long tail lasting for ~1ns. It is more like a triangular shape than a Gaussian. The full width at half the maximum was ~530ps in IR as shown in Figure 2.

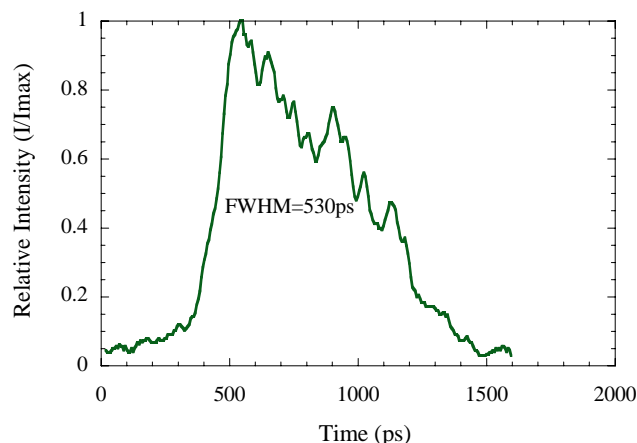


Figure 2. Shape of the main pulse recorded with an optical streak camera.

The main beams were focused from the opposite direction; three beams each side, in order to achieve uniform compression. The frequency doubled energy on target was ~200J each side contained in a focal spot of 3mm diameter. This roughly amounts to an irradiance of  $\sim 5 \times 10^{12} \text{W/cm}^2$  each side. The main target consists of either a 3 micron thick iron (Fe) or 6 micron

aluminium (Al) sandwiched between two thin layers of plastic (CH). The scattering data presented in this report is from the Al target.

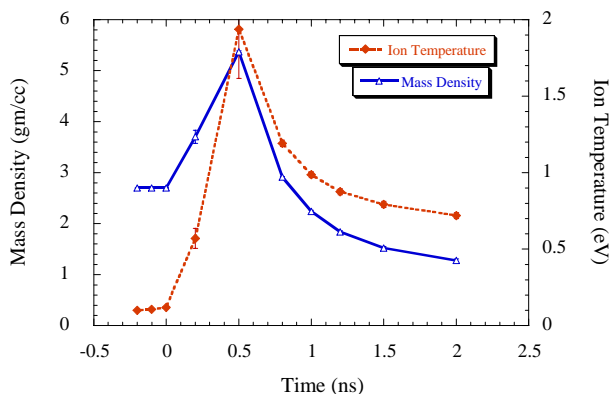
Beam 7 and 8, each delivering  $\sim 50\text{J}$  of IR in 80ps, were used for generating a x-rays source for probing the sample plasma. These two beams were frequency doubled and synchronously focused with f/5 lens onto a 3 micron thick Fe or Ti target to generate the probing backlighting x-ray beam with the dominant He- $\alpha$  ( $1S^2-1S2p^1P$  and satellites) line emission. The intensity on target was controlled by changing the focal spot dimension, varying from  $3 \times 10^{15} \text{ W/cm}^2$  to  $3 \times 10^{16} \text{ W/cm}^2$ . Random Phase Plates<sup>12)</sup> (RPP) were employed for some shots in order to see the effect of irradiation uniformity on the level of backlighter x-ray. The level of the back-lighter x-ray signal was monitored with the help of two flat-crystal spectrometers coupled to CCD system, one in the rear employing Si (111) and one in the front of the target making use of Ge(220) crystal.

After passing through an array of two pinholes, the probing x-ray beam was restricted to a narrow cone which determines the angular resolution of the experiment. However, high resolution restricts the incident signal to a lower signal level and a spread of  $6^\circ$  was employed as a compromise between resolution and signal level, using pinholes of 400 microns and 600 microns. The targets and pinholes were aligned offline with an external setup on a kinematic base. By varying the delay of beam 7 & 8 relative to the main beams, the back-lighter x-ray beam interacts with plasmas of varying conditions.

The Andor dual-chip x-ray CCD system cooled to  $-10^\circ\text{C}$  with nitrogen gas flow, was used in the photon counting mode<sup>13,14)</sup> to detect the scattered signal. Each chip has 2048 x 512 square pixels having dimension of 13.5 microns. The CCD was placed with its centre at a distance of 108mm from the sample plasma, thus covering a range of  $\sim 50^\circ$  to  $80^\circ$  scattered angle. Appropriate shielding was in place to block x-rays from the backlighter source hitting the CCD directly. A filtering of 72 micron Mylar, 250 micron Be, and 39 micron Al was employed in front of the dual chip CCD to eliminate to a great extent the unwanted radiation coming directly from the sample plasma. A calibration with Fe55 source (5.9keV) showed that Ti He-alpha lines could generate 126-130 counts with a resolution of about 6 counts (thermal broadening, for example). This limited our energy resolution to about 220eV.

## Results and Discussion

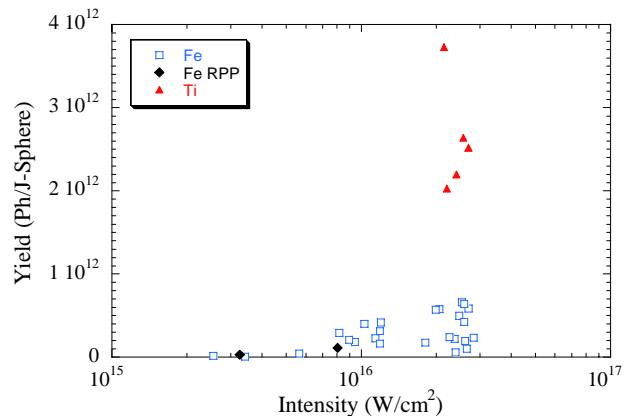
The 1-D Lagrangean hydrodynamics simulation code HYADES<sup>15)</sup> with the multi-group radiation transport package is used to simulate the expected conditions of the Al plasma at different time delays with respect to the peak of the pulse.



**Figure 3.** HYADES simulated conditions of laser-shock driven plasma.

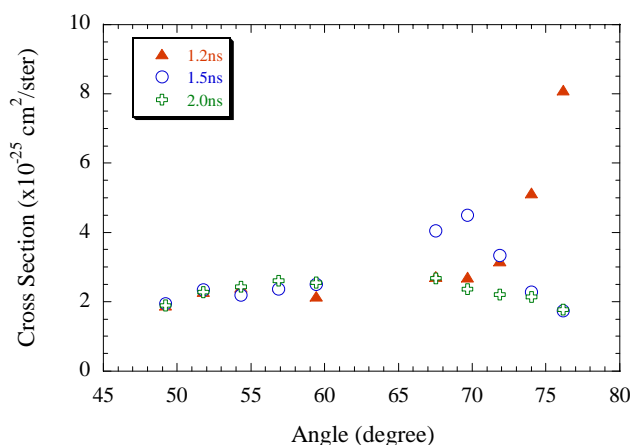
In Figure 3 we show the HYADES simulated average mass density and average ion temperature profile when a 6 micron thick Al target sandwiched between plastic (4.5 micron) is irradiated from the two opposite sides with 0.53 micron laser pulses at a peak intensity of  $5 \times 10^{12} \text{ W/cm}^2$ . We used the actual pulse shape shown in Figure 2 for these simulations. The zero on time scale coincides with the arrival of the peak of the main pulse. The error bars represent the statistical errors. The material is clearly compressed during the main pulse to about two times the solid density and about 2eV temperature. We probed the plasma at 1-2 ns after the peak of the pulse.

Figure 4 shows the level of He-alpha line emission (4749.2eV with a bandwidth of  $\sim 50\text{eV}$ ) recorded with the front spectrometer. In comparison with the energy resolution of our CCD system i.e. 220eV, this line emission could be considered as monochromatic. The graph shows a considerably higher yield of He- $\alpha$  emission with Ti (maximum  $\sim 4.0 \times 10^{12} \text{ Ph/J-Sphere}$ ) than obtained with Fe (maximum  $\sim 8.0 \times 10^{11} \text{ Ph/J-Sphere}$ ), as was expected. It also shows that irradiation uniformity using RPP's did not make any significant affect.



**Figure 4.** He-alpha line emission as a function of the backlighter beams intensity on target.

We used histograms of overlapping thirds of the CCD to achieve 5 data points separated by  $\sim 2$  degree each every shot. Due to the separation of the two chips, the central  $\sim 3.5$  degrees range was not covered in a single shot. Figure 5 shows the scattering cross-section measured as a function of scatter angle at various time delays. These data points were taken with Ti as a backlighter source and Al as the main plasma. The figure shows a scattering peak at an angle of  $\sim 70$  degrees for a delay of 1.5ns. At somewhat earlier time of 1.2ns with respect to the the main pulse, the trend of the data points indicates shifting of the peak towards a larger angle. This make sense as one would expect denser and hotter plasma at an earlier time before the peak, as can be seen from simulation in Figure 3, and hence shifting the peak towards the larger angle.



**Figure 5.** Ti He-alpha cross section measured with the dual chip x-ray CCD system as a function of the scattering angle.

Figure 5 also seems to suggest that the peak to base ratio decreases for the later time. At 2.0ns delay, the data does not show any peak. Either the peak data is missed in the angle region between the two chips or the peak to base ratio has become too small to be detected. Changing the position of the CCD system and adding another CCD to cover a bigger angular range may help resolve this issue. We also had two more data shots, one at 1ns and the other at 0.9ns w.r.t. the main pulse, but they do not show any peak, may be that the peak is further shifted and even a trend could not be seen. These data points are hence not shown in the Figure 4 for clarity purpose. Initially, we had concentrated our efforts on the scattering from Fe plasma using Fe backlighter; we simply did not have time to study the case of Al in detail. Although we tried Fe as a backlighter source for Fe, the level of Fe He-alpha emission was rather low as can be seen from Figure 4. This made the detection of the signal very difficult. The signal to noise level also hampered our efforts. Furthermore, K- $\alpha$  of Fe was also a problem.

While the scattering data obtained does not present a conclusive picture in terms of its usefulness for the direct measurement of plasma parameters, we have made progress in overcoming the technical problems associated with the setup of such a complex experimental setup. We feel that by increasing the level of Fe He-alpha emission, a scattered signal from the Fe-plasma could be recorded.

#### Acknowledgements

We would like to thank the target preparation staff at the Rutherford Appleton Laboratory. This work was supported by EPSRC grant EP/C001869/01.

#### References

1. T Guillot. *Science* **286**, 72 (1999)
2. L Spitzer. *Physics of Fully Ionized Gases*. Interscience, New York (1956)
3. H Brysk. *Plasma Physics* **16**, 927 (1974)
4. M W C Dharma-Wardana and F Perrot *Phys. Rev. E* **58**, 3705 (1998); erratum, *Phys. Rev. E* **63**, 069901-1
5. P Celliers *et al.*, *Phys. Rev. Lett.* **68**, 2305 (1992)
6. A Ng *et al.*, *Phys. Rev. E* **52**, 4299 (1995)
7. J Angulo-Gareta *et al.*, to be submitted
8. E Nardi *et al.*, *Phys. Rev. E* **57**, 4693 (1998)
9. E Nardi, *Phys. Rev. A* **43**, 1977 (1991)
10. J Chihara. *J. Phys. F: Met. Phys.* **17**, 295 (1987)
11. R M Stevenson *et al.*, *Optics Letters* **19**, 363 (1994)
12. Y Kato *et al.*, *Phys. Rev. Lett.* **53**, 1057 (1984)
13. D Riley *et al.*, *Phys. Rev. Lett.* **84**, 8 (2000)
14. D Riley *et al.*, *Phys. Rev. E* **66**, 046408 (2002)
15. J T Larsen J T and S M Lane, *J. Quant. Spectrosc. Radiat. Transfer* **51**, 179 (1994)